

1 **Adjustment of the iodine ICRP population pharmacokinetic**
2 **model for the use in thyroid cancer patients after**
3 **thyroidectomy**

4 Jan Taprogge^{1,2}, Lily Carnegie-Peake^{1,2}, Iain Murray^{1,2}, Jonathan I. Gear^{1,2} and Glenn
5 D. Flux^{1,2}

6 ¹ = Joint Department of Physics, Royal Marsden NHSFT, Downs Road, Sutton, SM2
7 5PT, United Kingdom

8 ² = The Institute of Cancer Research, 123 Old Brompton Road, London, SW7 3RP,
9 United Kingdom

10 * = corresponding author (jan.taprogge@icr.ac.uk)

11 Email addresses: Jan.Taprogge@icr.ac.uk, Lily.Carnegie-Peake@icr.ac.uk,
12 Iain.Murray@icr.ac.uk, Jonathan.Gear@icr.ac.uk, Glenn.Flux@icr.ac.uk

13 **Abstract**

14 **Introduction:** Biokinetic models developed for healthy humans are not appropriate to
15 describe biokinetics in thyroid cancer patients following thyroidectomy. The aim of this study
16 was to adjust the population model for iodine proposed by the International Commission on
17 Radiological Protection (ICRP) for the use in these patients.

18 **Method:** Rate constants of the ICRP publication 128 model for iodine were adjusted using
19 the population modelling software package Monolix to describe activity retention in whole-
20 body, thyroid, blood and protein-bound iodine observed in 23 patients. The new set of rate
21 constants was compared to the four uptake scenarios proposed in ICRP publication 128.

22 **Results:** Flow from the inorganic iodide in blood compartment into the first thyroid
23 compartment decreases to 0.15 day^{-1} compared to a value of 7.27 day^{-1} for the ICRP
24 publication 128 model with a medium uptake. The transfer from first to second thyroid
25 compartments and the outflow from the second thyroid compartment increases. An increased
26 turnover rate of extrathyroidal organic iodine is observed. The rate constant from inorganic
27 iodide in blood to kidney was also adjusted. Overall a good agreement was found between
28 the adjusted model and the activity retention in thyroid cancer patients.

29 **Conclusions:** The adjustment of population pharmacokinetic models to describe the
30 biokinetic properties of specific patient populations for therapeutic radiopharmaceuticals is
31 essential to capture the changes in biokinetics. The proposed set of rate constants for the
32 established ICRP publication 128 model can be used to more accurately assess radiation
33 protection requirements for the treatment of thyroid cancer patients using radioiodine.

34 **Keywords**

35 Radioiodine, biokinetic model, population model, thyroid cancer

36 **Introduction**

37 The International Commission on Radiological Protection (ICRP) has published biokinetic
38 models for many commonly used radiopharmaceuticals (1). These models have been used to
39 calculate dose coefficients for administration of radionuclides to patients. For patients
40 undergoing diagnostic examinations in nuclear medicine, absorbed doses to organs and
41 tissues are often calculated following the Committee on Medical Internal Radiation Dose
42 (MIRD) formalism (2) using dosimetric models with human computational phantoms and the
43 respective radiopharmaceutical biokinetic model (3). ICRP models are employed to assess
44 radiation protection requirements for patients in the nuclear medicine (NM) and molecular
45 radiotherapy (MRT) settings, and to provide radiation protection guidance to staff, patients and
46 caregivers (4-6).

47 A biokinetic model incorporating normal thyroid function (1, 7, 8) is not appropriate to describe
48 the use of radioiodine to treat residual tissue following partial or total thyroidectomy in thyroid
49 cancer patients. The biokinetics in these patients are significantly affected by partial or total
50 removal of the thyroid gland and the use of recombinant thyroid-stimulating hormone (rhTSH)
51 or thyroid hormone withdrawal (THW) (9). Excretion of radioiodine from the body is often
52 faster. ICRP publication 128 (ICRP128) provides iodine biokinetics for blocked, low, medium
53 and high thyroid function. No rate constants are provided in ICRP128 for patients following
54 thyroidectomy and activity retention in the thyroid remnant cannot be described with the
55 scenarios considered in ICRP128 (1).

56 Population pharmacokinetic modelling is used to study a substance's absorption, distribution,
57 metabolism, and excretion in a population of interest, such as a population with a specific
58 pathology. Population pharmacokinetic modelling using non-linear mixed effects (NLME)
59 allows for inter-patient variability by including both fixed and random effects (10). Simplistic
60 biokinetic models have been created using NLME for specific MRT patient cohorts (11-13),

61 although more complex models are required to include major organs for radiation protection
62 purposes.

63 A set of rate constants for the established ICRP128 biokinetic model was developed here for
64 radioiodine treatment of thyroid cancer following thyroidectomy. The rate constants of the
65 ICRP128 population biokinetic model were adapted using NLME to describe the
66 pharmacokinetics of radioiodine in a thyroid cancer patient cohort based on actual patient
67 data. These were compared to radioiodine pharmacokinetics in healthy individuals
68 represented by the established ICRP models.

69 **Method**

70 ***Radioiodine therapy patient data***

71 Thyroid remnant, whole-body and blood activity retention data were taken from a study by
72 Flux et al (14). 23 patients, 15 female and 8 male, were administered with a nominal activity
73 of 3000 MBq of ^{131}I -NaI. Patients were either not given thyroid hormone replacement between
74 surgery and ablation or thyroid hormones were discontinued for 14 days prior to radioiodine
75 treatment. No rhTSH was used in this study. The median age of patients was 41 years (range
76 18-70 years). Only patients with near-total or complete thyroidectomy were included in the
77 study. Furthermore, patients were excluded from the study if: they had distant metastases at
78 presentation, were treated with external beam radiotherapy or had been administered with
79 iodine-containing contrast, ^{123}I or ^{131}I tracers in the three preceding months before
80 administration of the therapeutic dose of ^{131}I .

81 Activity retention in the thyroid remnant was obtained from a minimum of three SPECT
82 acquisitions covering the neck and superior mediastinum using a Philips Forte gamma
83 camera. Scans were performed at nominally 24, 48 and 72 hours post administration. Two
84 patients had an additional scan at 96 hours and one patient had an additional scan at 32 hours.
85 Triple-energy-window scatter correction was used (15).

86 Blood samples were taken at 24, 48, 72 and 144 hours post administration. Protein bound
87 iodine (PBI) was extracted from blood. The major constituents of PBI are the thyroid
88 hormones, triiodothyronine (T3) and thyroxine (T4) (16, 17). Activity concentration of iodide
89 and PBI in blood were determined and converted to total activity in blood with the assumption
90 of a total blood volume of 5300 ml for adult males and 3900 ml for adult females (18). Whole-
91 body retention measurements were performed directly after administration (baseline value)
92 and at regular intervals until discharge of the patient.

93 All activity retention measurements were decay corrected back to the time of administration.
94 Further details about data acquisition and processing are provided in Flux et al (14).

95 ***Model adjustment***

96 Monolix 2019R2 (Antony, France: Lixoft SAS, 2019) was used for NLME modelling. The
97 structural base model of ICRP128, including the human alimentary tract model from ICRP
98 publication 100 (ICRP100) (19), was implemented as shown in Figure 1. A combined error
99 model was chosen for the residual errors with a log-normal residual error distribution (20).
100 Fitted rate constant distributions were assumed to be log-normally distributed to ensure
101 positivity of the values on all parameters. The ICRP128 model with the medium uptake rate
102 constants in the thyroid was used as a base model.

103 The iodine biokinetics in this patient cohort may differ from a healthy euthyroid population for
104 several reasons. Patients have undergone thyroidectomy and, as a result of THW, become
105 hypothyroid and have increased thyroid stimulating hormone (TSH) levels which regulate
106 sodium iodide symporter (NIS) expression in thyroid tissue (21).

107 The trapping rate of iodide into thyroid from blood depends in part on thyroid blood flow and
108 NIS expression. This process is described in the model by the rate constant from Blood 1 to
109 Thyroid 1. The altered blood supply to the thyroid remnant following thyroidectomy and
110 increased NIS expression resulting from high TSH (21) should affect the rate of iodide
111 trapping.

112 Several stages of organification of iodide to thyroid hormone are upregulated by increased
113 TSH levels (21-23). Additionally, Robertson et al found an increased organification rate in
114 thyrotoxic patients compared to euthyroid patients (22). Therefore, a change in the rate
115 constant from Thyroid 1 to Thyroid 2 may also be expected given the hypothyroid condition of
116 thyroid cancer patients under THW and increased TSH levels. The rate of secretion of thyroid
117 hormone (T3 and T4) from thyroid to blood, which is described by the rate constants from
118 Thyroid 2 to Blood 2, increases with TSH (8, 24).

119 Reductions in glomerular filtration rate (GFR) (25, 26), tubular secretion and re-absorption (26)
120 in hypothyroid patients have been reported. Durant et al measured increased serum
121 creatinine in patients under THW (27). Excretion of iodide by glomerular filtration is accounted
122 for by the rate constant from Blood 1 to Urinary bladder contents.

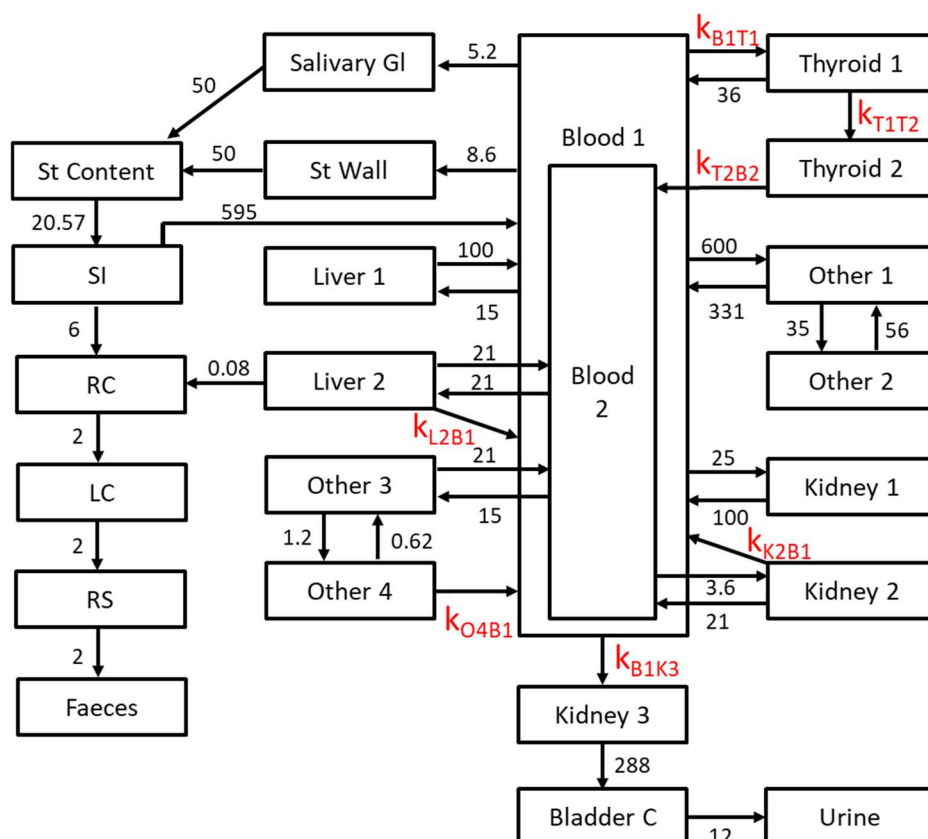
123 The ratio of T3 to T4 is elevated with rising TSH levels (24, 28-31). This is expected to result
124 in an increased turnover rate of extrathyroidal organic iodine due to the higher turnover rate
125 of T3 compared to T4 (32, 33). The turnover of extrathyroidal organic iodine is represented by
126 three rate constants, namely Kidney 2 to Blood 1, Liver 2 to Blood 1 and Other 4 to Blood 1.
127 The turnover is assumed to occur at the same rate from all three compartments (8).

128 The seven rate constants described above and indicated in red in Figure 1 were allowed to
129 vary in the fitting to the thyroid cancer patient data set. We could find no further evidence in
130 literature to support the adjustment of any of the remaining rate constants from the values
131 published in ICRP100 and ICRP128. It should be noted that in the current model voiding was
132 modelled as a constant excretion (8) which differs from the excretion model proposed by ICRP.

133 In the fit process, compartmental model rate constants were varied iteratively to achieve the
134 best agreement between activity retention observed in patients and predictions by the
135 compartmental model. For this purpose, thyroid activity retention in patients was taken to be
136 the sum of thyroid compartments 1 and 2 in the model. Furthermore, patient whole-body
137 activity retention was taken to be the sum of all compartments in the model excluding faeces

138 and urine. The blood and PBI activity retention data were assumed to correspond to Blood 1
 139 and Blood 2 compartments, respectively, with Blood 1 being the inorganic iodide and Blood 2
 140 the organic iodine in blood.

141



142

143 **Figure 1: The structural base model implemented in Monolix. Rate constants shown in red were tested**
 144 **during the model building process. In the base model, Blood 1 is the inorganic iodide in blood, Blood 2 is**
 145 **the organic iodine in blood, Thyroid 1 is the inorganic iodide in the thyroid, Thyroid 2 is the organic iodine**
 146 **in the thyroid, Kidney 1 is the inorganic iodide in kidneys, Kidney 2 is the organic iodine in kidneys, and**
 147 **Liver 1 is the inorganic iodide in liver, Liver 2 is the organic iodine in liver. Other 1 to Other 4 represent any**
 148 **tissues not specifically included in the model. Salivary GI are the salivary glands, St Wall is the stomach**
 149 **wall, St Contents are the stomach contents, SI are the small intestines, RC is the right-sided colon, LC is**
 150 **the left sided colon, RS is the rectosigmoid, Kidney 3 is an additional kidney compartment in the ICRP128**
 151 **model representing transfer to the bladder and Bladder C are the bladder contents. All rate constants are**
 152 **in units of day⁻¹.**

153 ***Model comparison to ICRP128***

154 Model predictions of the final population model were compared to individual observations in
155 patients. The biological retention predictions in each compartment of the final population
156 model were compared to the predictions of the ICRP128 base model.

157 **Results**

158 ***Model adjustment***

159 Rate constants of the updated ICRP128 population model developed here are presented in
160 Table 1 and compared to the respective rate constants of the ICRP128 base model. Flow from
161 the inorganic iodide in blood compartment (Blood 1) into the first thyroid compartment (Thyroid
162 1) decreases, the rate constant from inorganic iodide in thyroid (Thyroid 1) to organic iodine
163 in thyroid (Thyroid 2) approximately doubles and outflow from the second thyroid compartment
164 (Thyroid 2) increases by two orders of magnitude. Transfer from inorganic iodide in blood
165 (Blood 1) to Kidney 3 is found to be lower than in the ICRP128 model. The turnover rate of
166 extrathyroidal organic iodine, represented by the three rate constants from Kidney 2, Liver 2
167 and Other 4 to inorganic iodide in blood (Blood 1), is estimated to increase from 0.14 day^{-1} to
168 0.29 day^{-1} .

169

170

171

172

173

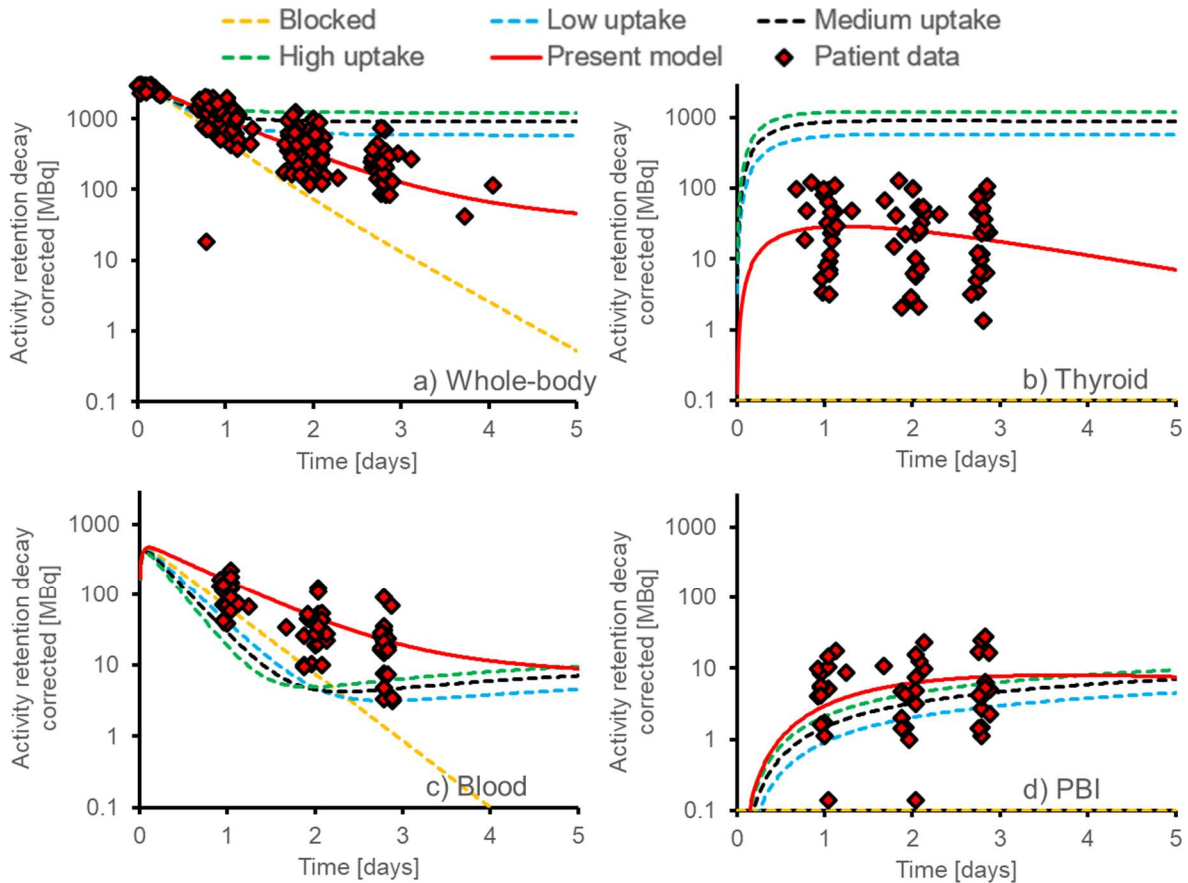
174 Table 1: Comparison of rate constants of the ICRP128 base model and the adjusted rate constants for the
 175 model developed here.

176

Rate constant	Flow between compartments (see Figure 1)	ICRP128 (medium uptake) [day^{-1}]	This model [day^{-1}]
k_{B1T1}	Blood 1 \rightarrow Thyroid 1	7.27	0.15
k_{T1T2}	Thyroid 1 \rightarrow Thyroid 2	95	181
k_{T2B2}	Thyroid 2 \rightarrow Blood 2	0.0077	0.50
k_{B1K3}	Blood 1 \rightarrow Kidney 3	11.83	6.87
$k_{K2B1}, k_{L2B1}, k_{O4B1}$	Kidney 2 \rightarrow Blood 1, Liver 2 \rightarrow Blood 1, Other 4 \rightarrow Blood 1	0.14	0.29

177

178 Figure 2 shows the predictions of the thyroid cancer patient model, compared to the
 179 predictions of the ICRP128 base model for the different uptake scenarios considered and the
 180 observed activity retention in patients. Predicted and measured activity retention in
 181 compartments has been corrected for physical decay. A good agreement was found between
 182 the predictions of the model and the activity retention measured in patients.

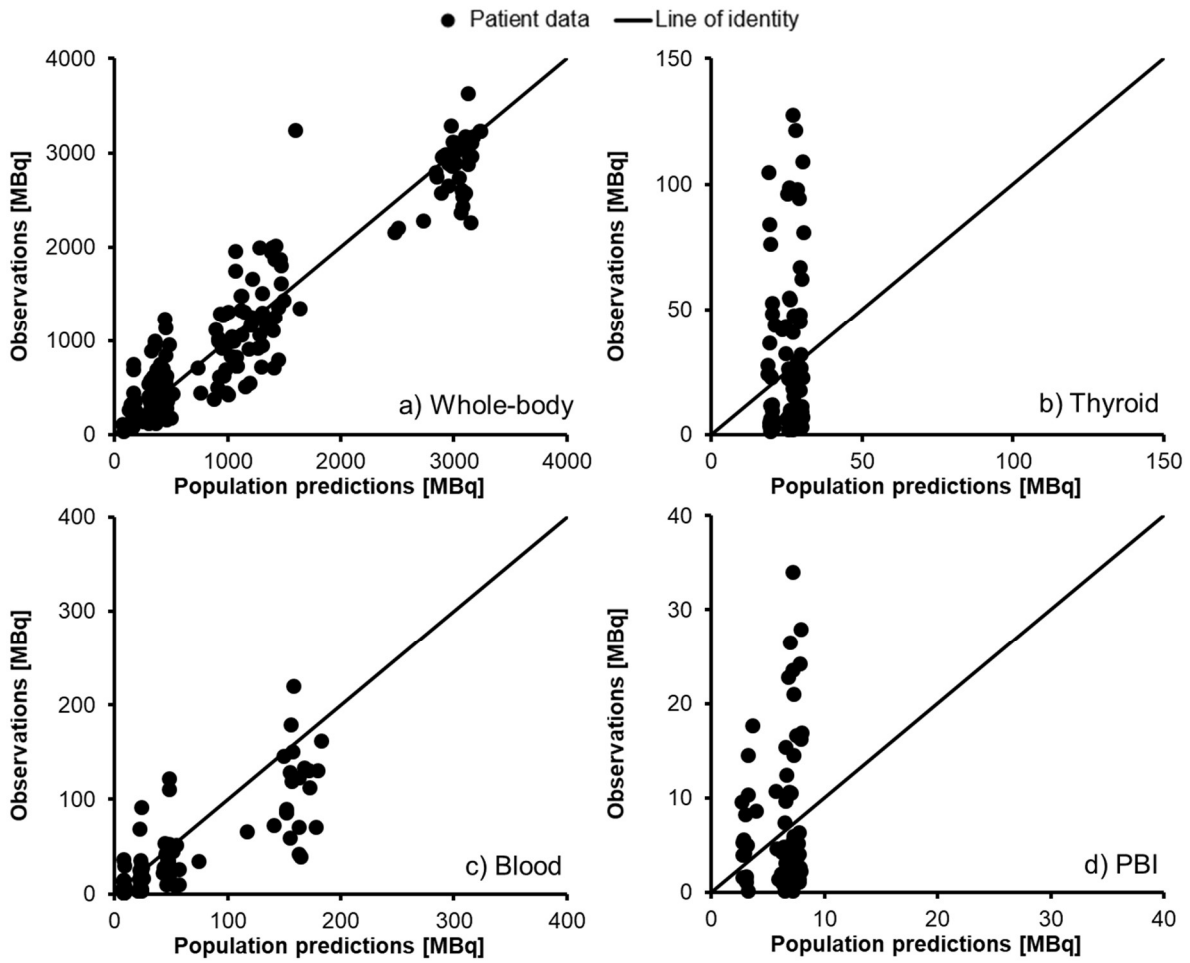


183

184 **Figure 2: Comparison of predictions of the final population model for thyroid cancer patients administered**
 185 **with 3000 MBq of $^{131}\text{I-NaI}$ (red solid line) obtained from a fit of rate constants k_{B1T1} , k_{T1T2} , k_{T2B2} , k_{B1K3} , k_{K2B1} ,**
 186 **k_{L2B1} and k_{O4B1} , of the ICRP128 base model, to patient data of Flux et al (14) (red diamonds). The predictions**
 187 **of the ICRP128 model for blocked thyroid (yellow dashed line), low (blue dashed line), medium (black**
 188 **dashed line) and high (green dashed line) uptake are presented for comparison. Activity retention was**
 189 **decay corrected back to the administration time and, therefore, biological retention is presented excluding**
 190 **physical decay.**

191 ***Model comparison to ICRP128***

192 Population model predictions were compared to the observed values in the 23 patients
 193 (Figure 2 and Figure 3). Predicted and observed whole-body and blood retentions are in good
 194 agreement, while the population model appears to perform less well to predict the variability
 195 in uptake in the thyroid remnant and PBI.



197

198 **Figure 3: Comparison of population model predictions to observations in patients for activity retention in**
 199 **(a) whole-body, (b) thyroid remnant, (c) blood and (d) PBI after a 3000 MBq ¹³¹I-NaI administration.**

200 As shown in Figure 2, the model with rate constants to describe a post-thyroidectomy thyroid
 201 cancer patient population shows a slower clearance from blood compared to ICRP128 while
 202 whole-body excretion is faster than the low, medium and high uptake scenarios in the
 203 ICRP128 model and slower than the blocked thyroid scenario. Thyroid activity retention peaks
 204 at 1.0% of the administered activity, which is markedly lower, compared to the low, medium
 205 and high uptake scenarios of ICRP128 of approximately 19%, 30% and 40% uptake in the
 206 thyroid. Maximum uptake in the thyroid remnant is predicted to occur around 29 hours, which
 207 is slightly faster than for the low, medium and high uptake scenarios of ICRP128 where peak
 208 uptake is observed between 42 to 54 hours after administration.

209 **Discussion**

210 Results presented here highlight the necessity of adjusting population pharmacokinetic
211 models to describe the biokinetic properties of specific patient populations for therapeutic
212 radiopharmaceuticals. Current ICRP models have been developed based on data from
213 healthy human or animal studies although biokinetic properties may change for patient
214 populations undergoing treatment. It has been shown here that the development of a patient-
215 specific population biokinetic model is feasible even with a limited number of patients and
216 measurements per patient.

217 The markedly faster urinary excretion predicted from this model, which has also been
218 observed in previous studies (34, 35), is an important factor in the MRT setting as it will affect
219 radiation protection guidance provided to staff, patients and caregivers. The model proposed
220 here with lower iodine uptake in the thyroid and faster urinary excretion compared to ICRP128,
221 provides a more accurate estimate of activity retention in this patient cohort. This could inform
222 radiation protection restrictions based on relevant national legislative requirements.

223 The observed increased rates of organification of iodide and secretion of thyroid hormones
224 are in agreement with literature evidence due to the high TSH caused by THW (21-24, 36). In
225 addition, the expected increase in turnover rate of extrathyroidal organic iodine identified from
226 literature (32, 33) was confirmed in the present model. Also in agreement with literature (25-
227 27), the excretion of iodide by glomerular filtration decreased.

228 A patient-specific pharmacokinetic model for dose assessment following radionuclide therapy
229 may require rate constants to be derived from either patient-specific covariates as part of a
230 physiologically-based pharmacokinetic (PBPK) model (37), or by adjustment of models to
231 patient-specific activity retention measurements (38). No patient-specific covariates were
232 added during the model development due to the small number of patients included in this
233 retrospective analysis. Inter-individual random effects, therefore, remain unexplained in the
234 current model. In the current state, the model is not able to make accurate predictions of

235 individual patient biokinetics, especially for activity retention in the thyroid remnant, as
236 demonstrated by Figure 3. EANM, EFOMP, EFRS, ESR and ESTRO have published a
237 common strategic research agenda for radiation protection in medicine (39), which includes
238 the refinement, validation and implementation of new biokinetic models for dosimetry in MRT.
239 A prospective study following a defined population modelling plan as defined in current best-
240 practice guidelines (40) should be performed to develop a more accurate model that could
241 potentially be used for individual patient biokinetic predictions which would enable
242 individualised radiation protection restrictions and could be used in the dose assessment. The
243 model presented here will be validated and extended using activity retention data and
244 covariates for 100 patients collected as part of a concurrent series of non-randomised, non-
245 blinded, prospective observational studies at four centres (Royal Marsden Hospital,
246 Universitätsklinikum Marburg, Universitätsklinikum Würzburg and Institute Universitaire du
247 Cancer de Toulouse Oncopole) as part of MEDIRAD Work Package 3 (41, 42).

248 Limitations of the current study include the relatively small patient sample and the fact that
249 data were only available for patients administered with a fixed activity of 3000 MBq, and
250 without rhTSH stimulation. Hänscheid et al (35) have shown that the effective half-time in
251 remnant thyroid tissue varies based on the patient preparation prior to radioiodine therapy,
252 namely rhTSH stimulation or THW. Furthermore, Ito et al presented results that the T3/T4 ratio
253 is lower in patients with total thyroidectomy during levothyroxine therapy when compared to
254 control (31). Therefore, a further model might be required for the sub-population of patients
255 administered under rhTSH stimulation. The model should also be validated for varying
256 amounts of administered activities. Nevertheless, the model has proven to accurately describe
257 the patient biokinetics for the patient cohort presented here.

258 **Conclusions**

259 A set of rate constants was developed for the established ICRP128 model to accurately
260 describe biokinetics of a thyroid cancer patient population with THW. The model developed

261 here can be used to more accurately assess radiation protection requirements for the
262 treatment of thyroid cancer patients using radioiodine.

263 **Acknowledgments**

264 NHS funding was provided to the NIHR Biomedical Research Centre at The Royal Marsden
265 and the ICR. The MEDIRAD project has received funding from the Euratom research and
266 training programme 2014-2018 under grant agreement No 755523. The RTTQA group is
267 funded by the National Institute for Health Research (NIHR). We acknowledge infrastructure
268 support from the NIHR Royal Marsden Clinical Research Facility Funding. This report is
269 independent research funded by the National Institute for Health Research (NIHR). The views
270 expressed in this publication are those of the author(s) and not necessarily those of the NHS,
271 the NIHR or the Department of Health and Social Care.

272 **Ethical statement**

273 Ethics committee approval and informed consent from all patients was obtained.

274 **References**

- 275 1. ICRP. Radiation dose to patients from radiopharmaceuticals: a compendium of current
276 information related to frequently used substances: ICRP Publication 128. Ann ICRP.
277 2015;44(2 Suppl):7-321.
- 278 2. Bolch WE, Eckerman KF, Sgouros G, Thomas SR. MIRD Pamphlet No. 21: A
279 generalized schema for radiopharmaceutical dosimetry—standardization of nomenclature. J
280 Nucl Med. 2009;50(3):477-84.
- 281 3. Andersson M, Johansson L, Eckerman K, Mattsson S. IDAC-Dose 2.1, an internal
282 dosimetry program for diagnostic nuclear medicine based on the ICRP adult reference voxel
283 phantoms. EJNMMI Res. 2017;7(1):88.

- 284 4. ICRP. Radiological protection in therapy with radiopharmaceuticals: ICRP Publication
285 140. Ann ICRP. 2019;48(1):5-95.
- 286 5. Bartlett ML. Estimated dose from diagnostic nuclear medicine patients to people
287 outside the Nuclear Medicine department. Radiat Prot Dosimetry. 2013;157(1):44-52.
- 288 6. Cho SG, Kim J, Song HC. Radiation safety in Nuclear Medicine procedures. Nucl Med
289 Mol Imaging. 2017;51(1):11-6.
- 290 7. Leggett R. An age-specific biokinetic model for iodine. J Radiol Prot. 2017;37(4):864-
291 82.
- 292 8. Leggett RW. A physiological systems model for iodine for use in radiation protection.
293 Radiat Res. 2010;174(4):496-516.
- 294 9. Taïeb D, Sebag F, Farman-Ara B, Portal T, Baumstarck-Barrau K, Fortanier C, et al.
295 Iodine biokinetics and radioiodine exposure after recombinant human thyrotropin-assisted
296 remnant ablation in comparison with thyroid hormone withdrawal. J Clin Endocrinol Metab.
297 2010;95(7):3283-90.
- 298 10. Mould DR, Upton RN. Basic concepts in population modeling, simulation, and model-
299 based drug development. CPT Pharmacometrics Syst Pharmacol. 2012;1(9):e6.
- 300 11. Areberg J, Jönsson H, Mattsson S. Population biokinetic modeling of thyroid uptake
301 and retention of radioiodine. Cancer Biother Radiopharm. 2005;20(1):1-10.
- 302 12. Barbolosi D, Summer I, Meille C, Serre R, Kelly A, Zerdoud S, et al. Modeling
303 therapeutic response to radioiodine in metastatic thyroid cancer: a proof-of-concept study for
304 individualized medicine. Oncotarget. 2017;8(24):39167-76.
- 305 13. Topić Vučenović V, Rajkovača Z, Jelić D, Stanimirović D, Vuleta G, Miljković B, et al.
306 Investigation of factors influencing radioiodine ¹³¹I biokinetics in patients with benign thyroid
307 disease using nonlinear mixed effects approach. Eur J Clin Pharmacol. 2018.
- 308 14. Flux GD, Haq M, Chittenden SJ, Buckley S, Hindorf C, Newbold K, et al. A dose-effect
309 correlation for radioiodine ablation in differentiated thyroid cancer. Eur J Nucl Med Mol
310 Imaging.. 2010;37(2):270-5.

- 311 15. Ogawa K, Harata Y, Ichihara T, Kubo A, Hashimoto S. A practical method for position-
312 dependent Compton-scatter correction in single photon emission CT. IEEE Trans Med
313 Imaging. 1991;10(3):408-12.
- 314 16. Acland JD. The interpretation of the serum protein-bound iodine: A review. J Clin
315 Pathol. 1971;24(3):187-218.
- 316 17. Clark F. Serum protein-bound iodine or total thyroxine. J Clin Pathol. 1975;28(3):211-
317 7.
- 318 18. ICRP. Basic anatomical and physiological data for use in radiological protection:
319 Reference values: ICRP Publication 89. Ann ICRP. 2002;32(3-4):1-277.
- 320 19. ICRP. Human alimentary tract model for radiological protection. A report of The
321 International Commission on Radiological Protection: ICRP Publication 100. Ann ICRP.
322 2006;36(1-2):25-327.
- 323 20. Proost JH. Combined proportional and additive residual error models in population
324 pharmacokinetic modelling. Eur J Pharm Sci. 2017;109:S78-S82.
- 325 21. Portulano C, Paroder-Belenitsky M, Carrasco N. The Na⁺/I⁻ symporter (NIS):
326 mechanism and medical impact. Endocr Rev. 2014;35(1):106-49.
- 327 22. Robertson JWK, Shimmins J, Horton PW, Lazarus JH, Alexander WD. Determination
328 of the rates of accumulation and loss of iodide and of protein-binding of iodine in the human
329 thyroid gland. In Dynamic Studies with Radioisotopes in Medicine. Proceedings of a
330 symposium. Rotterdam, 31 Aug-4Sept, 1970. International Atomic Energy Agency (IAEA):
331 IAEA; 1971:199-210.
- 332 23. Pesce L, Bizhanova A, Caraballo JC, Westphal W, Butti ML, Comellas A, et al. TSH
333 regulates pendrin membrane abundance and enhances iodide efflux in thyroid cells.
334 Endocrinology. 2012;153(1):512-21.
- 335 24. Tegler L, Gillquist J, Lindvall R, Almquist S, Roos P. Thyroid hormone secretion rates:
336 response to endogenous and exogenous TSH in man during surgery. Clin Endocrinol (Oxf).
337 1983;18(1):1-9.

- 338 25. Katz AI, Emmanouel DS, Lindheimer MD. Thyroid hormone and the kidney. *Nephron*.
339 1975;15(3-5):223-49.
- 340 26. Basu G, Mohapatra A. Interactions between thyroid disorders and kidney disease.
341 *Indian J Endocrinol Metab*. 2012;16(2):204-13.
- 342 27. Duranton F, Lacoste A, Faurous P, Deshayes E, Ribstein J, Avignon A, et al.
343 Exogenous thyrotropin improves renal function in euthyroid patients, while serum creatinine
344 levels are increased in hypothyroidism. *Clin Kidney J*. 2013;6(5):478-83.
- 345 28. Carlwe M, Schaffer T, Sjöberg S. Short-term Withdrawal of Levothyroxine, Induced
346 increase of thyroid-stimulating hormone and an increase ratio of triiodothyronine to thyroxine.
347 *Eur Endocrinol*. 2013;9(1):37-9.
- 348 29. Mortoglou A, Candiloros H. The serum triiodothyronine to thyroxine (T3/T4) ratio in
349 various thyroid disorders and after Levothyroxine replacement therapy. *Hormones (Athens)*.
350 2004;3(2):120-6.
- 351 30. Park SY, Park SE, Jung SW, Jin HS, Park IB, Ahn SV, et al. Free triiodothyronine/free
352 thyroxine ratio rather than thyrotropin is more associated with metabolic parameters in healthy
353 euthyroid adult subjects. *Clin Endocrinol (Oxf)*. 2017;87(1):87-96.
- 354 31. Ito M, Miyauchi A, Kang S, Hisakado M, Yoshioka W, Ide A, et al. Effect of the presence
355 of remnant thyroid tissue on the serum thyroid hormone balance in thyroidectomized patients.
356 *Eur Endocrinol*. 2015;173(3):333-40.
- 357 32. Colucci P, Yue CS, Ducharme M, Benvenga S. A Review of the pharmacokinetics of
358 levothyroxine for the treatment of hypothyroidism. *Eur Endocrinol*. 2013;9(1):40-7.
- 359 33. Nicoloff JT, Low JC, Dussault JH, Fisher DA. Simultaneous measurement of thyroxine
360 and triiodothyronine peripheral turnover kinetics in man. *J Clin Invest*. 1972;51(3):473-83.
- 361 34. Remy H, Borget I, Leboulleux S, Guilabert N, Lavielle F, Garsi J, et al. 131I effective
362 half-life and dosimetry in thyroid cancer patients. *J Nucl Med*. 2008;49(9):1445-50.
- 363 35. Hänscheid H, Lassmann M, Luster M, Thomas SR, Pacini F, Ceccarelli C, et al. Iodine
364 biokinetics and dosimetry in radioiodine therapy of thyroid cancer: procedures and results of

365 a prospective international controlled study of ablation after rhTSH or hormone withdrawal. J
366 Nucl Med. 2006;47(4):648-54.

367 36. Roelfsema F, Veldhuis JD. Thyrotropin secretion patterns in health and disease.
368 Endocr Rev. 2013;34(5):619-57.

369 37. Kletting P, Maaß C, Reske S, Beer AJ, Glatting G. Physiologically based
370 pharmacokinetic modeling is essential in 90Y-labeled Anti-CD66 radioimmunotherapy. PLOS
371 ONE. 2015;10(5):e0127934.

372 38. Andersson M, Mattsson S. Improved patient dosimetry at radioiodine therapy by
373 combining the ICRP compartment model and the EANM pre-therapeutic standard procedure
374 for benign thyroid diseases. Front Endocrinol (Lausanne). 2021;12(181).

375 39. EANM, EFOMP, EFRS, ESR and ESTRO. Common strategic research agenda for
376 radiation protection in medicine. Insights imaging. 2017;8(2):183-97.

377 40. Byon W, Smith MK, Chan P, Tortorici MA, Riley S, Dai H, et al. Establishing best
378 practices and guidance in population modeling: an experience with an internal population
379 pharmacokinetic analysis guidance. CPT Pharmacometrics Syst Pharmacol. 2013;2(7):e51.

380 41. Taprogge J, Leek F, Schurrat T, Tran-Gia J, Vallot D, Bardiès M, et al. Setting up a
381 quantitative SPECT imaging network for a European multi-centre dosimetry study of
382 radioiodine treatment for thyroid cancer as part of the MEDIRAD project. EJNMMI Phys.
383 2020;7(1):61.

384 42. MEDIRAD. <http://www.medirad-project.eu/>. Last accessed March 2021.